THE ASTROPHYSICAL JOURNAL, 534:482–489, 2000 May 1

Hα AND SOFT X-RAY BRIGHTENING EVENTS CAUSED BY EMERGING FLUX

Y. H. TANG, Y. N. LI, AND C. FANG
Department of Astronomy, Nanjing University, Nanjing 210093, China; yhtang@nju.edu.cn
G. AULANIER, B. SCHMIEDER, AND P. DEMOULIN
Observatoire de Paris, Département d'Astronomie Solaire et Planétaire, F-92195 Meudon, France
AND
T. SAKURAI
National Astronomical Observatory, Mitaka, Tokyo 181, Japan
Received 1998 April 24; accepted 1999 December 7

ABSTRACT

By using *Yohkoh* soft X-ray images, vector magnetograms, and Hα filtergrams, the brightening event that occurred on 1994 May 18 has been studied in detail. It occurred in a nearly potential large-scale magnetic configuration as shown by the comparison between the magnetic extrapolation (linear force-free field) and the large-scale soft X-ray loops. This event is related to the emergence of a new magnetic flux of about 3×10^{20} Mx. The impulsive enhancement of the emerging flux occurs about 20 minutes before the peaks of the Hα and soft X-ray brightening and lasts for about 10 minutes. This brightening may be a signature of reconnection taking place between the preexisting nonpotential loops and the new emerging small loops. The magnetic energy provided by reconnection is likely to be stored in the nonpotential loops and the emerging flux as implied by the vector magnetograms. By using the electron temperature and the electron density of the brightening event derived from the analysis of the *Yohkoh* data, an energy budget has been estimated. The result indicates that the energy needed can be reasonably provided by magnetic reconnection.

Subject headings: Sun: activity — Sun: magnetic fields — Sun: X-rays, gamma rays

1. INTRODUCTION

It is widely accepted that solar flares frequently occur in active regions of high magnetic shear (Hagyard et al. 1984) and complex magnetic topology (Mandrini et al. 1991). Nevertheless, we are still far from complete understanding of the detailed mechanism of energy build up and release. However, as major flares are generally too complicated to study, some small-scale flaring events, such as microflares and brightening events, can offer a better opportunity to understand the energy build up and release process. Recent high-resolution data makes the detailed study of small-scale flaring events possible and reliable. Thus, the study of small-scale flaring events is of importance in understanding the essential physical process.

In active regions where the magnetic topology is complex and the magnetic field is sheared, flares and flaring activities are known to be triggered by the motion and/or the emergence of magnetic flux. Such evolving magnetic fields can interact with the preexisting ones, and magnetic energy can be released there by magnetic reconnection (Heyvaerts & Hagyard 1991; Tsuneta et al. 1992). Depending on the amount of energy and on the magnetic topology involved, these processes lead to different dynamic phenomena such as flares, microflares, or X-ray bright points (Démoulin et al. 1992; Shimizu et al. 1992; Schmieder et al. 1996, 1997; van Driel-Gezstelyi et al. 1996; Benz et al. 1997) and surges or jets (Shibata et al. 1992; Schmieder et al. 1995).

It has recently been shown that flares can occur in regions where the overall magnetic field is nearly potential, despite the fact that, in such regions, large-scale magnetic reconnection cannot occur as there is no large-scale free magnetic energy. Leka et al. (1996) have shown that a newly emerging magnetic field can be more sheared than the preexisting ambient field, showing that such locally sheared fields could provide magnetic free energy that can be released in the corona by reconnection. A short-lived brightening event, which was close to an active region (Active Region 7722) but relatively isolated from other activity, was observed on 1994 May 18 with the multiwavelength data. Emerging flux was observed by Huairou station, which led to the brightening of small X-ray loops and Hα flaring points. In § 2 we describe the observations obtained at Huairou (active region magnetograms), at Kitt Peak (full-disk magnetograms), in Mitaka (Hα filtergrams), in Nanjing (white light), and with *Yohkoh*/SXT (soft X-ray images). An extrapolation of the photospheric magnetic field is described in § 3, where a comparison between extrapolated magnetic field lines and soft X-ray loops is given. In § 4 we analyze the data. § 5 presents a discussion, and § 6 gives a brief conclusion. With this multiwavelength study it is possible to estimate the energy budget, to determine the magnetic topology in order to understand whether the assumption of a reconnection model is consistent with the observations.

2. OBSERVATIONAL DATA

In May 1994, an active region, AR 7722, appeared on the solar disk at Carrington coordinates N8 L122. As it passed across the solar disk, a large sunspot with twin umbrae formed and became the most important sunspot on the solar disk. This brightening event, located in the southeast part of the sunspot, was observed on May 18 at N7.9 W4.4. The brightening was observed in soft X-ray and also in Hα at about 03:52 UT and disappeared after 04:50 UT (Fig. 1). Note that the scales of Hα and soft X-ray images are different (see the legend of Fig. 1). The coalignment of Hα and soft X-ray is shown in Figure 2.

The *Yohkoh* soft X-ray telescope (SXT; Tsuneta et al.

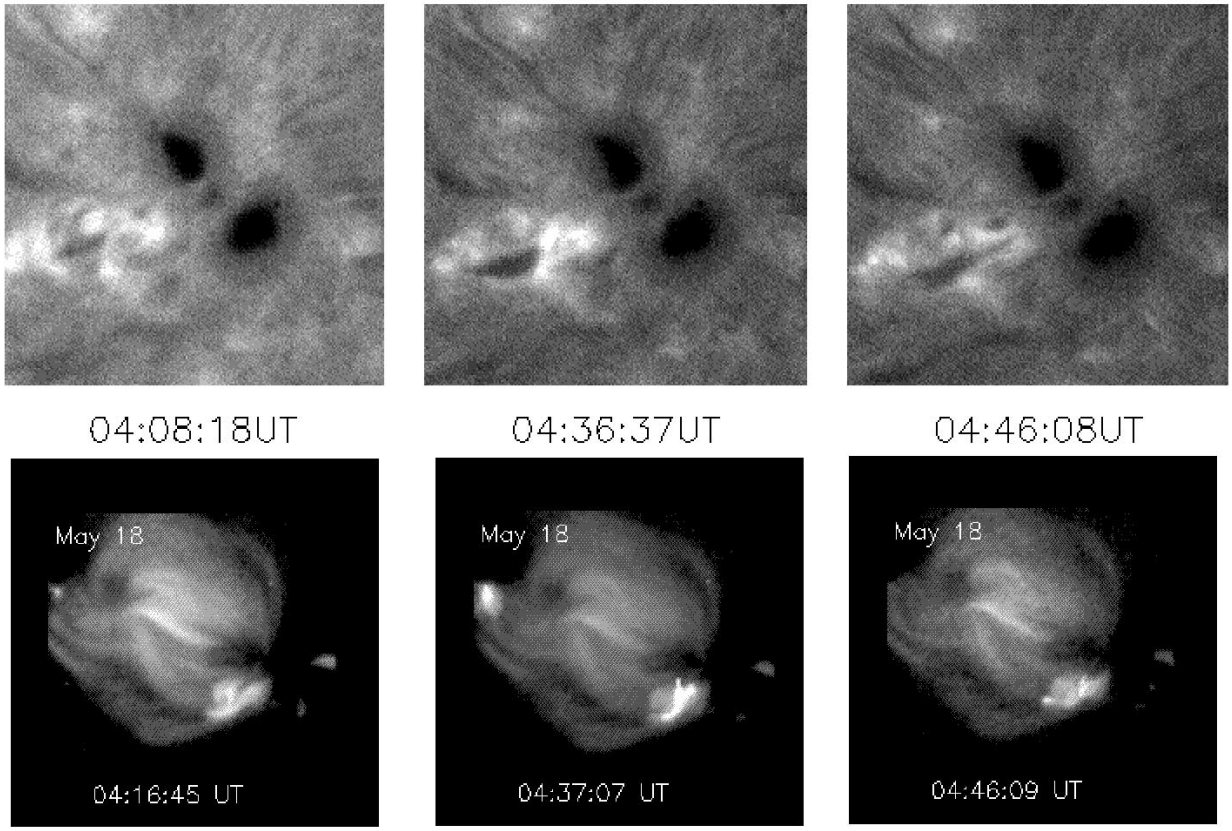

FIG. 1.—Temporal evolution of the brightening event observed in (*bottom panel*) the soft X-ray by *Yohkoh*/SXT and (*top panel*) in the Hα line on 1994 May 18. The brightening events are located southeast of the large sunspot. The field of view of the soft X-ray images is 128 × 128 pixels (313″ × 313″). The field of view of the Hα images is 120″ × 109″. North is up and east is to the left.

1991) obtained soft X-ray images (using the Al 0.1 μm, Al 12 μm, and AlMg filters) for both the active region and the whole solar disk, which were recorded with 128 × 128 pixels and 512 × 512 pixels, respectively. The pixel size of partial frame images is 2.″45 × 2.″45. Some SXT images near the maximum of the brightening are saturated. We did not use these saturation images to evaluate the variation of the relative intensities of the brightening nor to obtain the electron temperature and the emission measure. Vector magnetic field and sunspot observations were made at the Huairou Station of Beijing Astronomical Observatory of China. A CCD with 512 × 512 pixels was used to cover a field of view of 316.″6 × 217.″6 (Zhang & Ai 1986). There are eight magnetograms, including five chromospheric (using hydrogen Hβ λ4861.34) and three photospheric ones (Fe I λ5324). Hα filtergrams were obtained with 512 × 480 pixels covering a field of view of 345″ × 323″ at the National Astronomical Observatory of Japan (Sakurai et al. 1992). Since the Hα images were recorded on a video disk with a constant sensitivity, the evolution of the brightening can be analyzed. Eighteen frames for the May 18 event were digitized (including images taken at Hα line center and at Hα ± 0.6 Å). The daily solar full-disk picture was drawn at the solar tower of Nanjing University (see Huang et al. 1995 for a description of the instrumentation), giving the positions and the shapes of sunspots. The diameter of the solar image is 19.8 cm. The full-disk magnetograms were taken from Kitt Peak. All observational data are listed in detail in

TABLE 1

LIST OF OBSERVATIONAL DATA

Wavelength	Instrument	Pixel Size (arcsec)	Day	Observation
Magnetograms.....	magnetograph (Huairou)	~0.5	May 18	three local photospheric vector magnetograms: 03:57, 04:42, 05:57 UT
Magnetograms.....	magnetograph (Huairou)	~0.5	May 18	five chromospheric magnetograms: 04:09:05, 04:12:53, 04:15:43, 04:19:48, 04:23:18 UT
Magnetograms.....	magnetograph (Kitt Peak)	1	May 17	full disk: 15:47 UT
Soft X-ray	*Yohkoh*/SXT	2.45	May 18	full disk: 03:47–04:48 UT
Soft X-ray	*Yohkoh*/SXT	2.45	May 18	partial frame: 03:47–04:47 UT
Hα filtergrams	flare telescope (Mitaka)	0.67	May 18	03:52–04:46 Ut
White light	solar tower (Nanjing University)	...	May 16–19	one every day (sunspot positions)

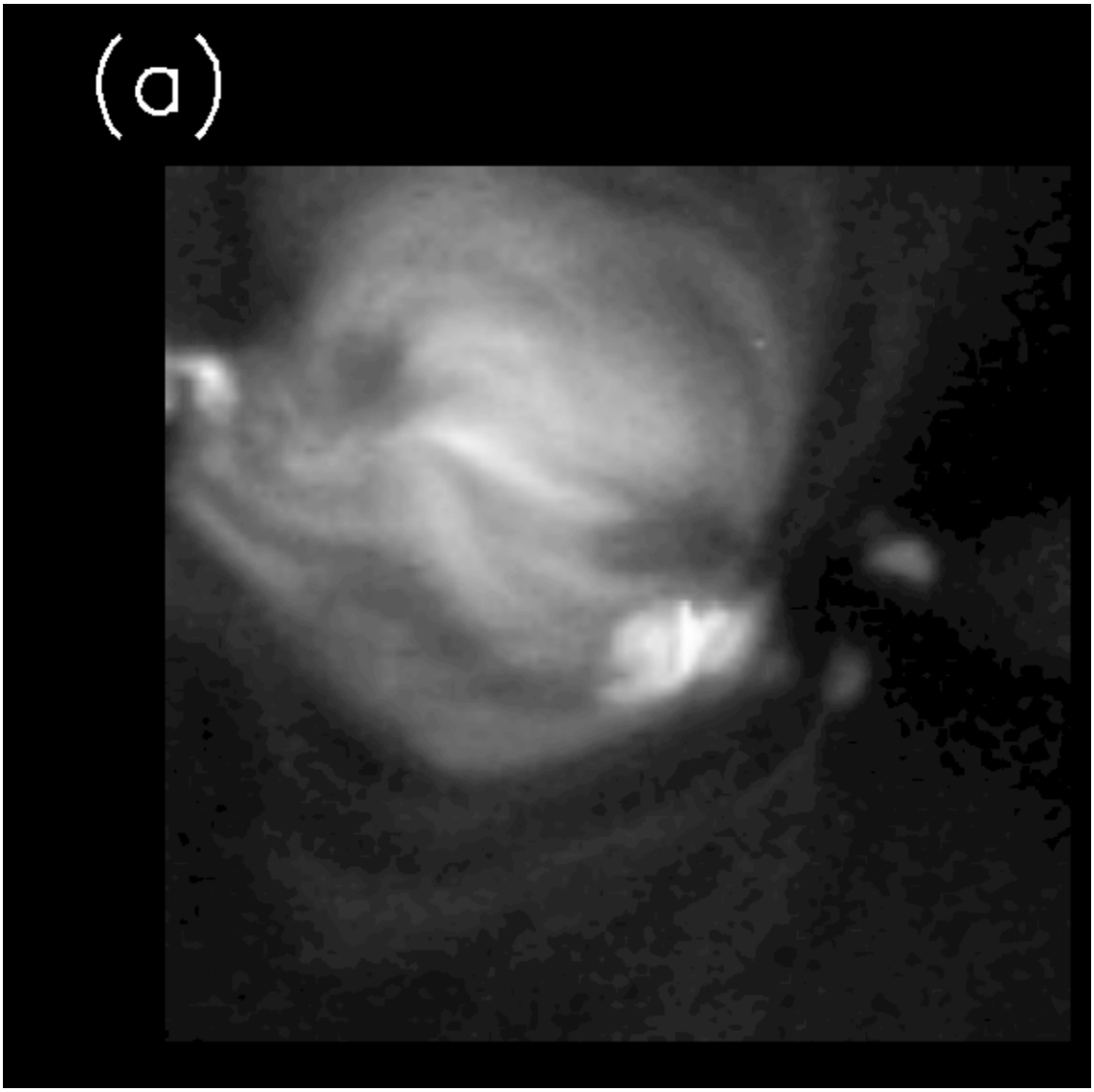

FIG. 2.—Large-scale view comparison of the magnetic configuration obtained with a linear force-free field extrapolation of the Kitt Peak magnetogram (May 17, 15:47 UT) of AR 7722 with observations. (*a*) Soft X-ray image taken on May 18 at 04:35:31 UT with *Yohkoh*/SXT and (*c*) corresponding magnetic field lines for $\alpha = -6.3 \times 10^{-3}$ Mm^{-1}. Isocontours of 50, 200, 600, 1000, and 2000 G for the photospheric vertical field (*solid lines*) and respective negative values (*dashed lines*) are shown. (*b*) Corresponding Hα image from Mitaka on May 18 at 04:36:37 UT. North is up and east is to the left.

Table 1. No substantial radio emission was detected. *Yohkoh* HXT also did not register any hard X-ray emission.

3. EXTRAPOLATION OF THE PHOTOSPHERIC MAGNETIC FIELD

In this section, we derive the large-scale (whole active region) and the small-scale (around the brightening region) magnetic configuration in order to find the magnetic environment in which the flux emergence occurred. This is realized by comparing extrapolated magnetic field lines to soft X-ray loops.

Using a magnetogram, our aim is to extrapolate the photospheric longitudinal field (B_l) to the corona. In order to find the large-scale magnetic environment, we chose to use one of the full-disk magnetograms produced by Kitt Peak. We could easily coalign the full-disk magnetogram and the *Yohkoh*/SXT full-frame image and select a box (500 × 500 Mm) to compare the extrapolated magnetic field lines and the soft X-ray loops.

In the solar upper atmosphere, the force-free field assumption is well satisfied, so the field can be described by the following equation:

$$\nabla \times \boldsymbol{B} = \alpha \boldsymbol{B} \, . \tag{1}$$

We used a linear approximation, where α is a constant. Then the solution of equation (1) can be expressed as a combination of harmonics for the magnetic field. The extrapolation method is derived from the one described by Alissandrakis (1981). We used a Cartesian system of coordinates, where z refers to the height and (x, y) to the photospheric plane at $z = 0$. Knowing the B_z component of the field constrains the two other components. Taking into account the fact that the studied region is near the disk center, we suppose that the longitudinal photospheric field

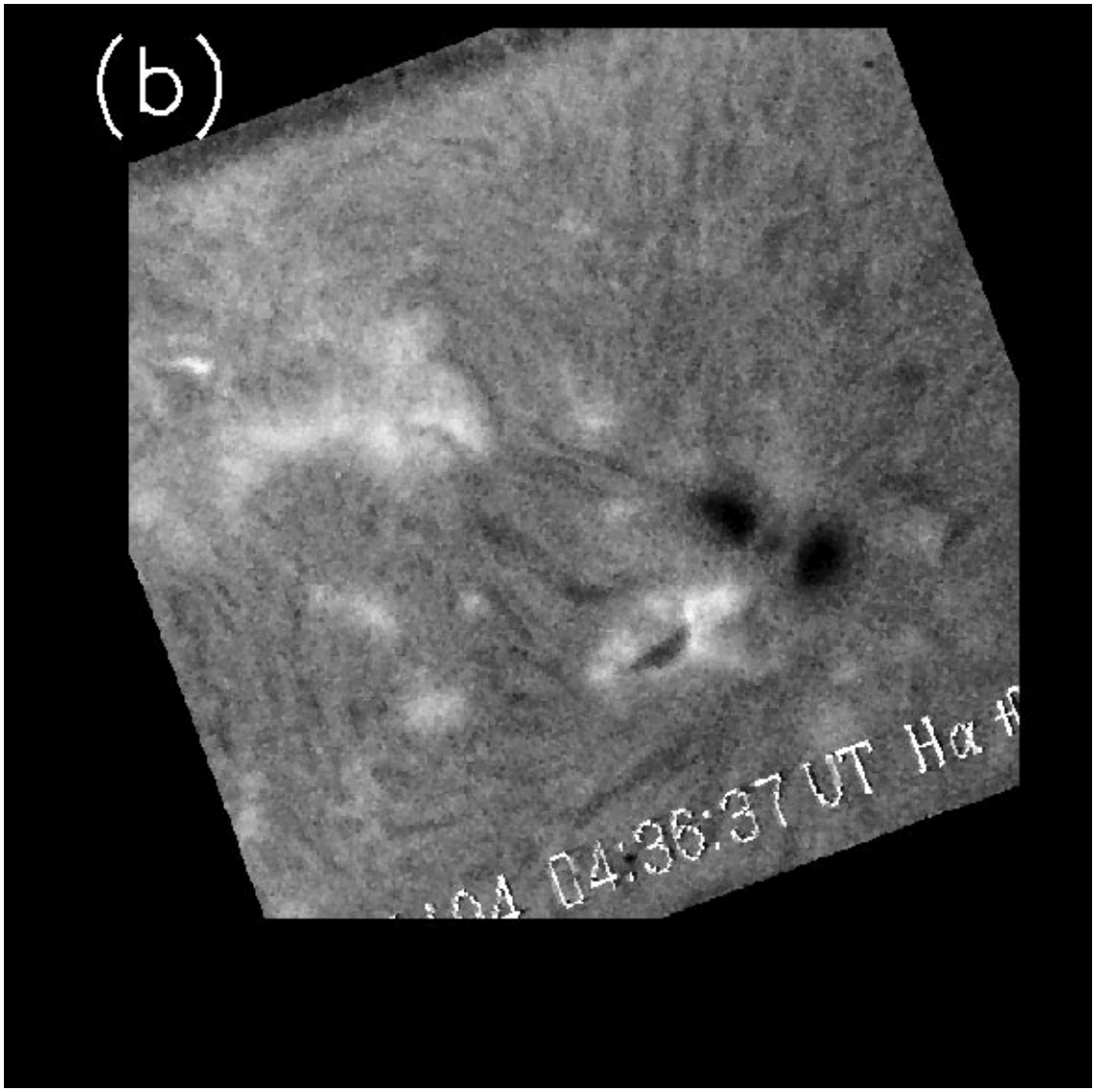

FIG. 2.—*Continued*

is vertical. Such an assumption corresponds mainly to neglecting the curvature of the sun in the selected box, which leads to an error of 2 Mm at the edges of the box. The differences between imposing B_z and B_l and more details on this method can be found in Démoulin et al. (1996).

For a given value of α, we obtained the three components of $\boldsymbol{B}$ everywhere in the computational box. In order to fit the soft X-ray loops with a sample of extrapolated field lines, we need to find the value of α or equivalently the average shear in the active region. In order to do so, we extrapolated the photospheric field with a given α and drew a number of field lines. Making some variations on the α value, which is a free parameter in our extrapolation code, we found a relatively good match between the high-altitude X-ray loops and the computed field lines for one value (see Figs. 2*a* and 2*c*). This value of α is not significantly different from zero, implying that the large-scale magnetic field is nearly a potential one.

Figure 3 shows the superposition of the partial soft X-ray images (*top:* at 03:54:23 UT, near the onset of the brightening; *bottom:* at 04:42:21 UT, after the maximum of the brightening), the magnetograms (Huairou data; *top*, at 03:57:44 UT; *bottom*, at 04:42:30 UT), and the extrapolated potential magnetic field lines (at the height of small X-ray loops, $\sim 10^9$ cm) around the brightening region. It is especially interesting to note that before the brightening, the small X-ray loops were not oriented along the potential field lines although the large-scale magnetic field is nearly a potential one (Fig. 3, *top*), and the brightening appears in these nonpotential loops. However, after the maximum of the brightening, the small loops became oriented more or less along the potential field lines (Fig. 3, *bottom*). This fact implies that the nonpotential energy was released to heat the plasma as indicated by the enhanced soft X-ray emission during the brightening event.

4. ANALYSIS OF THE DATA

4.1. *Coalignment*

The locations of the brightenings have been obtained by using the full-disk SXT and white-light images. Then we used the sunspot images to determine the necessary parameters (rotation angle, scale ratio for data reduction, etc.) for the coalignment of the soft X-ray images, the Huairou magnetograms, and the Hα filtergrams (Fig. 2). The precision of the coalignment is estimated to be $\sim 3''$. For direct compari-

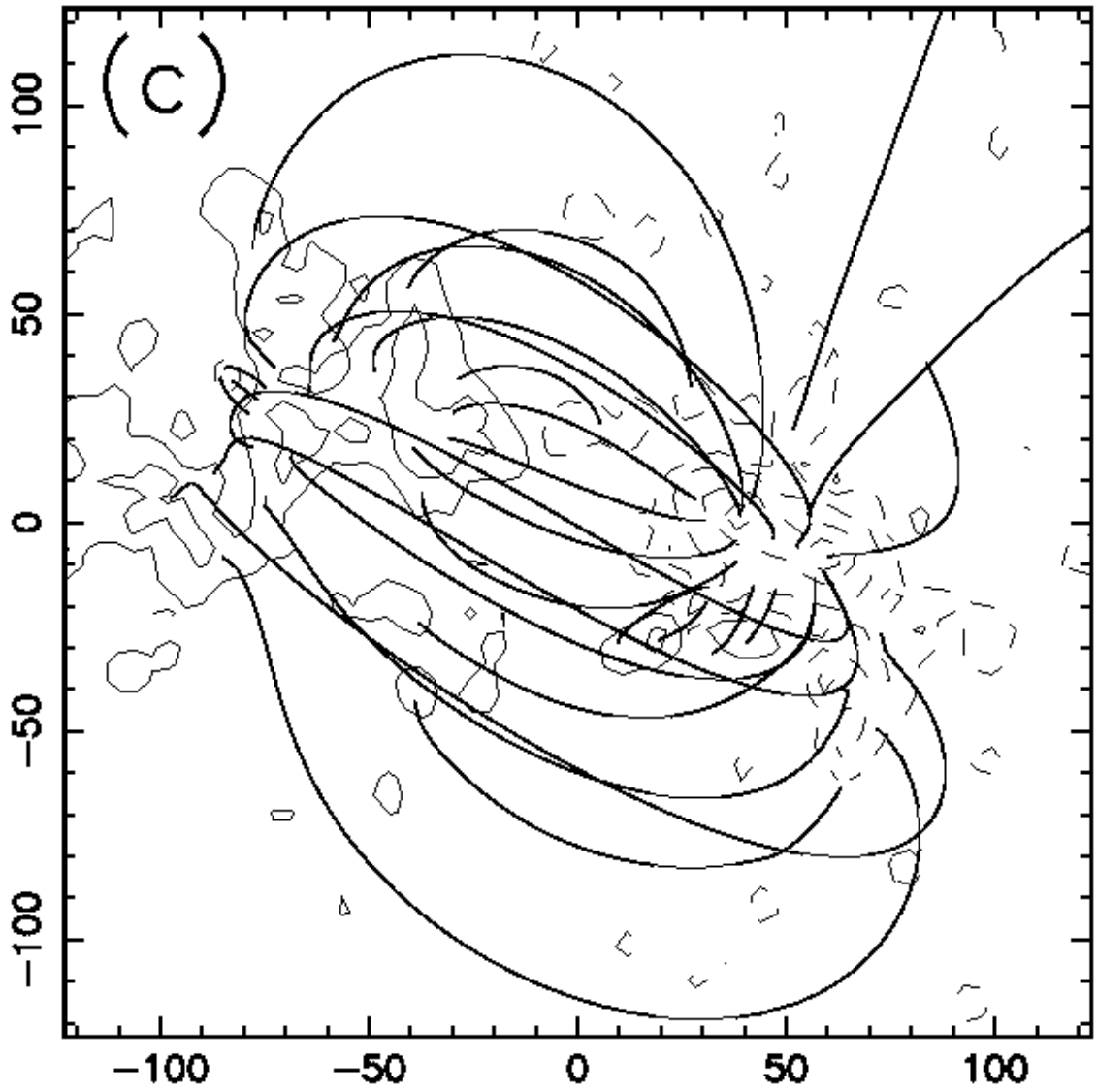

FIG. 2.—*Continued*

son, we projected the soft X-ray images and Hα images onto the magnetograms and found that the bright points of soft X-ray and Hα are located in the middle of the three points marked A, B, and C in Figures 4 and 5.

4.2. *Emerging Magnetic Flux*

In order to understand the cause of the brightening, a detailed study of the small-scale emerging flux is necessary. Eight magnetograms have been analyzed; five of them are chromospheric ones, and three are photospheric vector magnetograms. Since the absolute calibration of the chromospheric magnetogram is questionable, we only analyzed the relative variation of the chromospheric magnetic flux. Figures 4 and 5 show two vector magnetograms of the photosphere and three longitudinal magnetograms of the chromosphere, respectively. It can be seen in Figure 4 that the amplitude of the transverse magnetic field is of the same order as the longitudinal magnetic field. Moreover, it is obvious that the direction of the transverse field rotates by 30°–40° during the interval 03:57–05:57 UT in the middle part of the triangle ABC, which is larger than the uncertainty (about 15°–20°). From Figure 4 the magnetic flux of the photosphere at each of the points A and B has been found to be about 3×10^{20} Mx at 03:57 UT (the magnetic flux had an average uncertainty of 10%).

The relative variations of the chromospheric magnetic flux at the points A and B have been measured (Fig. 5). By use of the images taken at Hα line center, Hα relative intensities averaged over 5×8 pixels around the brightest point have been measured. The relative error in the measurement was estimated to be less than 2%–3%. Using the light-curve procedure in the *Yohkoh* software, we have also obtained the soft X-ray relative intensity of the brightening region in a box of 3×4 pixels around the brightest point. Figure 6 gives the temporal evolution of the Hα and soft X-ray relative intensities for the event. The relative variation of the chromospheric magnetic flux is also plotted in Figure 6. It can be seen that the peaks of the Hα and soft X-ray brightenings appeared almost at the same time. The precision of the cotemporal behavior is estimated to be within ± 40 s. It can also be seen that the emerging flux increases about 20 minutes before the peak of the Hα and soft X-ray brightening. The duration of the event (midpoint of rise to midpoint of decline) is estimated to be about 10 minutes.

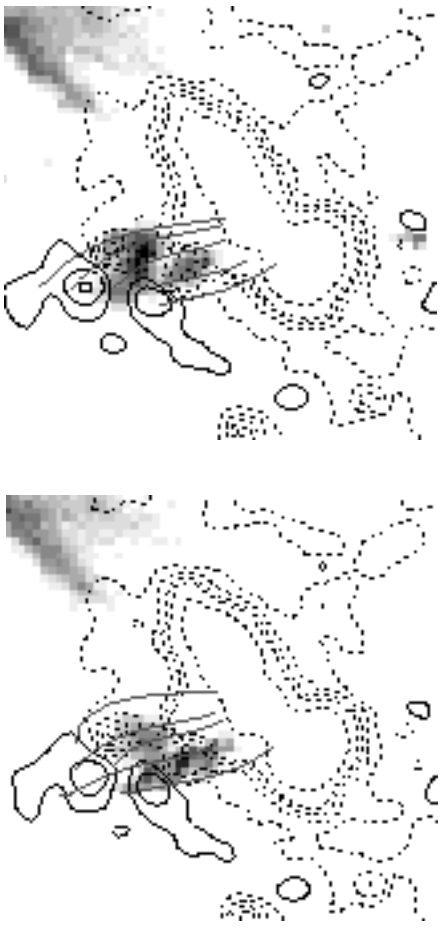

FIG. 3.—Superposition of the soft X-ray images (gray scale, *top:* at 03:54:23 UT; *bottom:* at 04:42:21 UT) and the photospheric longitudinal magnetograms (contours are the same as in Fig. 2; *dashed lines* correspond to negative polarity and *solid lines* to positive polarity) around the emerging flux region at (*top*) 03:57:44 UT and (*bottom*) 04:42:30 UT, as well as the extrapolated potential magnetic field lines (*solid lines* linking the positive and negative polarities). The field of view is 64 × 64 pixels. North is up and east is to the left.

4.3. *Determination of T_e and n_e*

The SXT aboard *Yohkoh* provided partial-frame images during the period of the event. The partial-frame images were coaligned and organized to form two parallel data cubes, one with a thin filter (Al 0.1 μm) and one with a thick filter (AlMg). The sensitivity of the filters allows one to determine a temperature in a range between 10^6 and 10^7 K with an accuracy of about $\pm 10\%$ (Hara et al. 1992). With the filter-ratio method, both the electron temperature T_e and the emission measure EM as a function of time were determined for a selected box, which is 3 × 4 pixels around the soft X-ray brightest point. We obtained a mean electron temperature $T_e = 5 \times 10^6$ K, with a maximum temperature around 8×10^6 K, and $EM \sim 5 \times 10^{45}$ cm^{-3}. Assuming that the thickness d along the line of sight, being equal to the width of the measured box, equals 6×10^8 cm, the volume of the X-ray emission at the brightest point can be estimated as $\Delta V = \Delta S \times d$, where ΔS is the size of the measured box. We have $\Delta S = 3 \times 10^{17}$ cm^2. Thus, the electron density can be obtained as $n_e = (EM/\Delta V)^{1/2} \sim 5 \times 10^9$ cm^{-3}.

Comparing these values to those corresponding to the long stable loops overlying the central part of the active region (see Fang et al. 1997), we found that T_e in the brightening event is higher ($T_e = 5 \times 10^6$ K) than that at the top of the stable loops, which is about 3×10^6 K. The electron density is the same as that at the top of the stable loops.

5. DISCUSSION

As mentioned above, using the filter-ratio method, we determined the temperature and the emission measure of the brightening event. For the following discussion we use an electron temperature of about 5×10^6 K and an electron density of 5×10^9 cm^{-3} to give a rough estimate of the energy loss of the small soft X-ray loops, which is related to the brightening. The energy loss of the loops is mainly due to radiative cooling and heat conduction. The radiative cooling rate is given by (Nagai 1980)

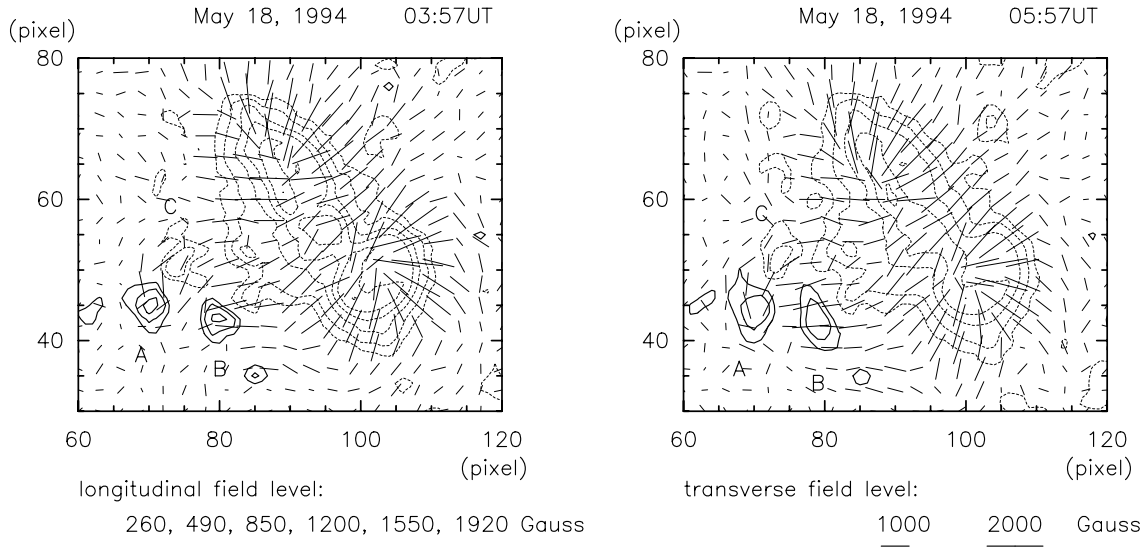

FIG. 4.—Photospheric vector magnetograms around the emerging magnetic flux region bounded by points A, B, and C at (*left*) 03:57 UT and (*right*) 05:57 UT. Pixel size is 1.″86 × 1.″70. The transverse field magnitude is represented by the length of vectors without arrows and the longitudinal field by the contours: dashed lines correspond to negative polarity and solid lines to positive polarity.

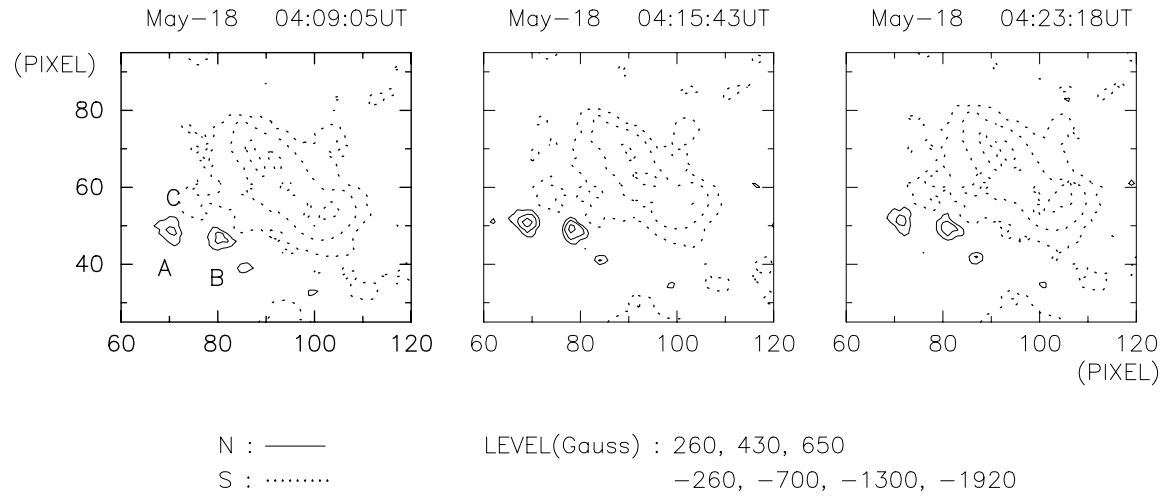

FIG. 5.—Chromospheric longitudinal magnetograms around the emerging magnetic flux region at (*left*) 04:09:05, (*middle*) 04:15:43, and (*right*) 04:23:18 UT. The pixel size is the same as in Fig. 4.

$$R = n_e n_{\rm H}\, f(T) \approx n_e^2\, f(T)\,, \tag{2}$$

and

$$\log f(T) = -0.604 \log T - 18.333,\ (10^6{\rm K} < T < 10^7{\rm K})\,, \tag{3}$$

where $n_{\rm H}$ and n_e are the hydrogen and electron densities, respectively. Thus, $R \approx 1 \times 10^{-3}$ ergs cm^{-3} s^{-1}. The energy loss from the chromosphere cannot be measured because the Hα intensity is a relative one. Thus, the energy loss by radiation is a lower limit. The energy loss due to heat conduction can be roughly estimated by

$$\nabla \cdot \boldsymbol{q} = \nabla \cdot (C_0\, T^{5/2} \nabla T) \approx \frac{C_0\, T^{7/2}}{(L/2)^2}\,, \tag{4}$$

where $C_0 = 10^{-6}$ and L is the length of the loop (Švestka 1987). Assuming that the loops are semicircular with two footpoints separated by a distance of 1.4×10^9 cm as measured on the soft X-ray images, we find the length of each loop to be about 2×10^9 cm. Using equation (4), we get

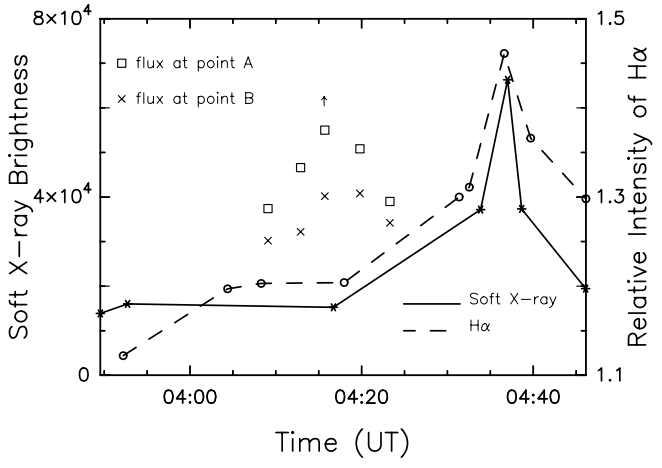

FIG. 6.—Temporal evolution of the relative intensities of soft X-ray (*solid line*) and Hα line center (*dashed line*) for the brightening event on 1994 May 18. The relative variations of chromospheric magnetic flux at the points A (*squares*) and B (*crosses*) are also given. The arrow indicates the peak time of the emerging flux.

$\nabla \cdot \boldsymbol{q} \approx 2.8 \times 10^{-1}$ ergs cm^{-3} s^{-1}. Then the radiative cooling at the coronal level is negligible, and the total energy loss rate would be $R + \nabla \cdot \boldsymbol{q} \approx 2.8 \times 10^{-1}$ ergs cm^{-3} s^{-1}. The section of the small loop is supposed to be constant and is estimated to be 3.8×10^{16} cm^2 from the kernel diameter of the small loop. Then the volume of the loop is $\sim 7.6 \times 10^{25}$ cm^3. Thus, the total energy loss rate would be 2.1×10^{25} ergs s^{-1}. If we take the duration of the brightening to be about 10 minutes, the total energy loss of the X-ray brightening is about 1.3×10^{28} ergs.

What is the cause of the brightening? Here we propose a scenario based on the above observations and estimate how much energy could be provided. According to overlapping X-rays, Hα brightening points, and the magnetogram, we found that the brightening points were located above the middle of the region bounded by the three points marked A, B, and C (see Fig. 4 or Fig. 5). Figure 3 demonstrates that the preexisting loops are nonpotential. In Figure 5 the enhancement of the chromospheric magnetic flux at the footpoints can also be seen. All these facts imply that the brightening of the Hα and soft X-ray may be caused by the reconnection between the preexisting nonpotential loops and the small emerging loops.

Let us roughly test this scenario. We suppose that all the magnetic field is annihilated and only one-half of the released energy is offered to heat the plasma. The rate of the energy release provided by the reconnection can be estimated as

$$\frac{dW}{dt} = l^2 v\, \frac{B^2}{8\pi}\,, \tag{5}$$

where l is the length and the width of the reconnection region, v the inflow speed, and B the magnetic field in the reconnection region. If we take the extrapolated potential field at the height of the small X-ray loops ($\sim 10^9$ cm) as the one in the reconnection region, then B is around 100 G. It is generally assumed that the magnetic flux tubes are completely diffused in the corona, so the filling factor is not so important for estimating the magnetic field intensity in the corona. Thus, the value of 100 G is to some extent a "mean" value. We take $l = 1.5 \times 10^8$ cm, $t = 10^3$ s, and $B = 100$ G as the characteristic values; then the Alfvén velocity $V_{\rm A} = 2.5 \times 10^8$ cm s^{-1}. As the maximum dimen-

sionless annihilation rate (see Petschek 1964) is about 0.1–0.01, so we take $v = 0.05V_A$. Thus, the total energy heating the plasma and provided by the reconnection would be 5×10^{25} ergs s^{-1}. Thus, the magnetic reconnection is likely to provide enough power to explain the estimated energy loss.

6. CONCLUSION

The conclusions of this paper can be briefly summarized as follows.

1. From the linear force-free field extrapolation of the photospheric field based on a Kitt Peak magnetogram, we deduce that the magnetic field of AR 7722 is almost potential because large-scale field lines computed in potential configuration closely match the large soft X-ray loops (Fig. 2). However, the small-scale X-ray loops around the brightening region are not oriented along the potential field lines before the brightening (Fig. 3, *top*).

2. From the location of the brightenings (Fig. 2) the brightening events seem to be related to the new emerging flux. The energy of the events seems to come from the reconnection between the new emerging loops and the preexisting small X-ray loops, which were nonpotential.

3. The new emerging magnetic flux at the footpoints of the small loops increases in strength about 20 minutes before the intensity peaks of the Hα and soft X-ray brightening. It lasts about 600 s. The photospheric magnetic flux at the footpoints of the small loops is about 3×10^{20} Mx.

4. The brightenings of the Hα and soft X-ray reach their maximum at almost the same time with an accuracy of about ± 40 s.

5. Using the filter-ratio method, we determined the temperature and the electron density for the brightening events: $T_e = 58 \times 10^6$ K, and $n_e = 5 \times 10^9$ cm^{-3}.

6. We found an order of magnitude agreement between the energy loss from the soft X-ray brightening by radiative and conductive processes ($\simeq 10^{28}$–10^{29} ergs), and the energy could be provided by the reconnection.

Two authors (T. Y. H. and F. C.) would like to express their sincere gratitude to the National Astronomical Observatory of Japan and the CNRS of France for supporting their stays in Tokyo and Paris, respectively. Thanks are also due to the Beijing Astronomical Observatory and K. Harvey (NOAO) as well as the *Yohkoh* team for kindly providing the magnetic field data and soft X-ray images, respectively. This work was partly supported by the National Natural Science Foundation of China under Major Project 19791090 and 49990451, as well as RFDP. B. S. thanks CNRS and NSFC for support and Nanjing University for kind hospitality. We would like much to thank the referees for their very valuable comments and suggestions on improving both the science and the language. Thanks are also due to M. Woodard and Lidia van Driel-Gezstelyi for manuscript corrections.

REFERENCES

Alissandrakis, C. E. 1981, A&A, 100, 197
Benz, A. O., Krucker, S., Acton, L. W., & Bastian, T. S. 1997, A&A, 320, 993
Démoulin, P., Bagalá, L. G., Mandrini, C. H., Hénoux, J. C., & Rovira, M. G. 1996, A&A, 325, 305
Démoulin, P., Hénoux, J. C., & Mandrini, C. H. 1992, Sol. Phys., 139, 105
Fang, C., Tang, Y. H., Ding, M. D., Zhao, J. W., Sakurai, T. & Hiei, E. 1997, Sol. Phys., 176, 267
Hagyard, M. J., Smith, J. R., Teuber, D., & West, E. A. 1984, Sol. Phys., 91, 115
Hara, H., Tsuneta, S., Lemen, J. R., Acton, L. W., & McTiernan, J. M. 1992, PASJ, 44, L135
Heyvaerts, J., & Hagyard, M. 1991, Proc. Chantilly Meeting, Dynamics of Solar Flares, ed. E. Priest & B. Schmieder (Paris: Obs. de Paris DASOP), 1
Huang, Y. R., Fang, C., Ding, M. D., Gao, X. F., Zhu, Z. G.,Ying, S. Y., Hu, J., & Xue, Y. Z. 1995, Sol. Phys., 159, 127
Leka, K. D., Canfield, R. C., McClymont, A. N., & van Driel-Gesztelyi, L. 1996, ApJ, 462, 547
Mandrini, C. H., Démoulin, P., Hénoux, J. C., & Machado, M. E. 1991, A&A, 250, 541
Nagai, F. 1980, Sol. Phys., 68, 357
Petschek, H. E. 1964, in AAS-NASA Symp. on Physics of Solar Flares, ed. W. N. Hess (NASA SP-50), 425
Sakurai, T., et al. 1992, PASJ, 44, L7
Schmieder, B., Aulanier, G., Démoulin, P., Roudier, T., Nitta, N., & Cauzz,i G. 1997, A&A, 325, 1213
Schmieder, B., Rovira, M., Simnett, G. M., Fontenla, J. M., & Tandberg-Hanssen, E. 1996, A&A, 308, 957
Schmieder, B., Shibata, K., van Driel-Gesztelyi, L., & Freeland, S. 1995, Sol. Phys., 156, 245
Shibata, K., et al. 1992, PASJ, 44, L173
Shimizu, T., Tsuneta, S., Acton, L. W., Lemen, J. R., & Uchida, Y. 1992, PASJ, 44, L147
Švestka, Z. 1982, Sol. Phys., 108, 411
Tsuneta, S., et al. 1991, Sol. Phys., 136, 37
Tsuneta, S., Hara, H., Shimizu, T., Acton, L., Strong, K., Hudson, H., & Ogawara, Y. 1992, PASP, 44, L63
van Driel-Gesztelyi, L., et al. 1996, Sol. Phys., 163, 145
Zhang, H. Q., & Ai, G. X. 1986, Acta Astron. Sinica, 9, 266